



ELSEVIER

Available online at www.sciencedirect.com

SCIENCE @ DIRECT®

JOURNAL OF
ENVIRONMENTAL
RADIOACTIVITY

Journal of Environmental Radioactivity 65 (2003) 329–355

www.elsevier.com/locate/jenvrad

Prediction of the fate of radioactive material in the South Pacific Ocean using a global high-resolution ocean model

Douglas R. Hazell ^a, Matthew H. England ^{*a}

^a *University of New South Wales, School of Mathematics, Centre for Environmental Modelling and Prediction, New South Wales 2052, Australia*

Received 22 August 2001; received in revised form 9 April 2002; accepted 20 May 2002

Abstract

We investigate the release of radioactive contaminants from Moruroa Atoll in a global high-resolution off-line model. The spread of tracer is studied in a series of simulations with varying release depths and time-scales, and into ocean velocity fields corresponding to long-term annual mean, seasonal, and interannually varying scenarios. In the instantaneous surface release scenarios we find that the incorporation of a seasonal cycle greatly influences tracer advection, with maximum concentrations still found within the French Polynesia region after 10 years. In contrast, the maximum trace is located in the southeast Pacific when long-term annual mean fields are used. This emphasizes the importance of the seasonal cycle in models of pollution dispersion on large scales. We further find that during an El Niño/Southern Oscillation (ENSO) event reduced currents in the region of Moruroa Atoll result in increased concentrations of radioactive material in French Polynesia, as direct flushing from the source is reduced. In terms of the sensitivity to tracer release time-rates, we find that a gradual input results in maximum concentrations in the near vicinity of French Polynesia. This contrasts the instantaneous-release scenarios, which see maximum concentrations and tracer spread across much of the South Pacific Ocean. For example, in as little as seven years radioactive contamination can reach the east coast of Australia diluted by only a factor of 1000 of the initial concentration. A comparison of results is made with previous studies. Overall, we find much higher concentrations of radionuclides in the South Pacific than has previously been predicted using coarser-resolution models.

© 2002 Elsevier Science Ltd. All rights reserved.

Keywords: Moruroa; Mururoa; Ocean model; South Pacific; Radioactive tracer; French Polynesia

* Corresponding author. Fax: +61-2-9385-7123.

E-mail address: M.England@unsw.edu.au (M.H. England).

1. Introduction

The tropical South Pacific Ocean continues to be exposed to the risk of radioactive contamination in the marine environment. Underground nuclear weapons testing in French Polynesia was conducted from 1975 until 1996 at Moruroa Atoll and the closely neighboring Fangataufa Atoll (IAEA, 1998). The contaminated material resulting from these tests contained within the geological structure of these atolls is a potential source of pollution (Ribbe & Tomczak, 1990, hereafter RT90).

It is appropriate to determine the extent and magnitude of such potential pollution using the best available methods. To this end, an off-line tracer model was developed using the velocity fields of a high-resolution global ocean model. Previous studies have been undertaken of the advection and dispersion of radioactive material from Moruroa Atoll (e.g., Ribbe & Tomczak, 1990; Tomczak & Herzfeld, 1998; Mittelstaedt et al., 1999; Lazar & Rancher, 1999; hereafter LR99). However, these studies were subject to a number of simplifications. For example, they each adopted a limited ocean domain requiring unrealistic side boundary conditions. The RT90 study suffered from a very low model resolution, inadequate for simulating realistic ocean currents. The Tomczak and Herzfeld (1998) model was the only study to address seasonal variations, and this was on a limited regional scale. The previous studies all neglect the possible role of interannual ocean variability. In this paper we plan to address each of these limitations using a global-domain, high-resolution tracer model with time-varying ocean flow patterns.

The aims of this study are: (1) To develop a global off-line tracer model of eddy-permitting resolution, and (2) to predict the potential fate of radioactive material released from Moruroa Atoll, improving on previous studies by using a higher resolution, a global domain, and incorporating seasonal and interannual ocean variability.

To avoid excessive complexity and preserve the generality of the results of this study, three important assumptions are made. As in all previous studies (except RT90) the decay of radioactive isotopes has not been incorporated into the tracer model. The high number of radionuclides present (32 species were identified by one study; IAEA, 1998) and their relative abundance creates enormous complexity in the incorporation of decay rates and decay products into the study results. Radionuclides are therefore considered as a passive tracer (physically constant in time). This assumption allows the model to be used for any radionuclide with a half-life greater than around one year (over shorter time-scales non-linear mixing effects could be important). The second assumption is that the background concentration of radionuclides in the South Pacific Ocean is set to zero. Results therefore describe the additional concentration of radionuclides originating from the Moruroa release site. The third assumption is that the leakage of tracer is uniformly and instantaneously mixed within the release grid box (which has horizontal dimensions of ~ 40 km by 40 km). Again, this assumption is common to previous studies. As our model has relatively fine resolution, however, the impact of this third assumption is much less than that of the previous studies. The turnover time for water within Moruroa Atoll is of the order of 100 days (Tartinville et al., 1997; Deleersnijder et al., 1997; the atoll lagoon dimensions are approximately 25 km by 10 km). Flushing rates of water

outside the lagoon will be more rapid due to local tidal currents and open ocean wind effects. As such, it may be assumed that our simulations would lead a real world leakage scenario by about one year when the release is gradual and within the atoll lagoon. For a catastrophic event that involves partial destruction of the lagoon, such as a landslide or earthquake, the model lead-time could be somewhat less than a year.

The release of tracers from Moruroa Atoll is simulated at different depths in the water column and at two different time rates (instantaneous and gradual). We also incorporate different climate scenarios to gain some indication of the effects of seasonal and interannual variability on tracer advection. All of the simulations are carried out over ten years. Finally, a comparison of the results of our study is made with two earlier simulations that used coarse resolution (Ribbe and Tomczak, 1990) and a limited domain model (Ribbe and Tomczak, 1990 and Lazar and Rancher, 1999), along with constant background flow fields.

Throughout this paper the spelling of the name of the atoll at which the majority of French nuclear tests was conducted is 'Moruroa', as opposed to 'Mururoa'. The former spelling is more closely associated with its origins in the local Maohi languages; the latter can be attributed to a typographical error made by a French cartographer (MacIellan and Chesneaux, 1998).

2. The off-line tracer model

An 'off-line tracer model' is one in which only the tracer is a prognostic variable; other quantities such as velocity fields, mixing and convection are inputs into the model. The off-line simulation of the oceanic transport of tracer requires the combination of two computational tools. The first is an ocean general circulation model (OGCM) that defines the grid resolution and velocity of ocean currents. The second is a tracer dispersion model, which computes the effects of advection and mixing on the tracer using a prescribed source function and the velocity data set from the OGCM.

2.1. The ocean general circulation model

The velocity fields used to determine the advective transport of the tracer in this study are obtained from the Parallel Ocean Climate Model (POCM), which is a descendent of the Semtner and Chervin (1992) half-degree global model. The more recent version includes a finer resolution (order quarter of a degree), the removal of 'deep-ocean restoring' of temperature and salinity values, and the inclusion of a free surface (Stammer et al., 1996). The model simulates ocean circulation for the majority of the world's oceans, excluding the Arctic Ocean (to avoid grid convergence problems). It is forced using the twice-daily wind stress fields smoothed to three-day fields from the European Centre for Medium-range Weather Forecasting (ECMWF) model reanalyzed over a 20-year period from 1979 to 1998. The algorithms used to simulate ocean dynamics are adapted from the Geophysical Fluid

Dynamics Laboratory (GFDL) Modular Ocean Model (Bryan, 1969; Cox, 1984; Pacanowski et al., 1991).

The POCM has a global mean horizontal resolution of approximately one quarter-degree latitude and longitude over a Mercator grid. Due to converging meridians at the poles, fine resolution is defined at high latitudes. The north–south resolution varies from 0.1° at high latitudes to 0.4° in the tropics. Zonal resolution is 0.4° , which corresponds to a range of 15 km at high latitudes to 44 km in the tropics. The model divides the vertical dimension of the ocean into 20 geopotential depth levels. These range in thickness from 25 m in the upper 100 m up to 400 m at the bottom level (5500 m).

The advection fields used in our study are derived from the monthly mean velocities of the full 20-year POCM run. This allows for computation of the long-term annual, monthly-mean, and interannually varying velocity fields used in the tracer experiments.

2.2. Simulated ocean dynamics

Fig. 1a shows the long-term annual mean surface circulation of the South Pacific Ocean in the POCM. For clarity, vectors of ocean current direction are only shown over a coarse 4° grid. The major surface currents of the South Pacific Ocean are well represented by the model, including the subtropical anticyclonic gyre, the equatorial current system and the western boundary current (the East Australian Current, EAC). The overall transport is summarized in the mass transport stream function shown in Fig. 1b. This shows depth-integrated flow in Sverdrups ($1 \text{ Sv} = 10^6 \text{ m}^3 \text{ sec}^{-1}$). Clearly apparent is the subtropical gyre in the South Pacific Ocean, with the EAC transporting 30 Sv polewards. Near Moruroa, whilst surface flow is eastward, the interior ocean circulation from 260–1000 m depth is westward.

We have compared surface currents from the POCM with available observational data from the NOAA/AOML Drifter Data Assembly Centre. This data was collected across the Pacific Ocean from August 1995 to May 2001 and has been integrated over a 5° grid to give an estimate of the observed annual mean circulation (Fig. 2). The model reproduces the large-scale direction and magnitude of circulation in the South Pacific. Most relevant to our study, the eastward surface drift simulated in the POCM in the region of Moruroa Atoll is confirmed by the drifter data (Fig. 2). Other major features of the surface circulation such as the EAC and the equatorial current system also show agreement between model and observations. Data is insufficient to make a more detailed comparison between climatological observed and modeled circulation in the region of Moruroa Atoll. It may also be noted that the construction of the observational diagram (Fig. 2), by spatial averaging on a 5° by 5° grid, can alias a number of features captured by the POCM (e.g., the South Equatorial Counter Current).

Direct measurements of the circulation in the South Pacific Ocean at depths below the wind-driven surface layer are very sparse. Reid (1986) estimated the circulation at depth using available measurements of tracers (temperature, salinity, oxygen, silica and helium-3) and density. The POCM simulation at depth is in general agreement

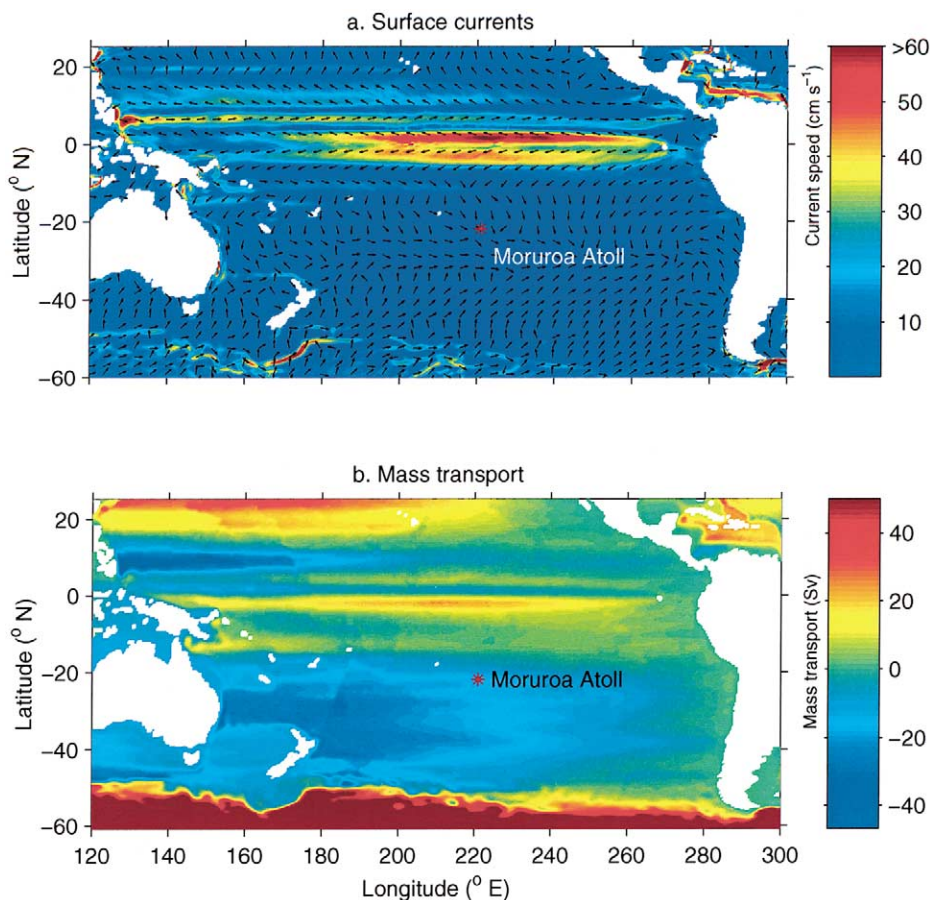


Fig. 1. Modeled South Pacific Ocean circulation: (a) surface current speed (cm sec^{-1}) and direction, (b) depth-integrated mass transport streamfunction (Sv, $1 \text{ Sv} = 10^6 \text{ m}^3/\text{sec}$). In (a), vectors indicate direction only and are drawn over a coarse 4° grid. In (b), negative values indicate an anti-clockwise circulation in the Southern Hemisphere.

with the Reid (1986) flow patterns. In particular, at depths of 300 m to 1400 m, currents in the tropical South Pacific flow in a broad westward direction, with the southward-flowing western boundary current closing the gyre circulation. The southward extent of the interior gyre flow increases with depth as observed. Seasonal variability is reduced in the oceanic mid-depths, being driven by larger-scale, long-term thermohaline forces and geostrophy (Tomczak and Godfrey, 1994). The effects of interannual climate variations can, however, be apparent at mid-depths, with a decrease in westward current velocity occurring during the 1982–1983 El Niño/Southern Oscillation (ENSO) event.

Fig. 3 shows spatially averaged horizontal ocean currents over a 5° grid centered at Moruroa Atoll during January, July, on the annual mean, and during an ENSO

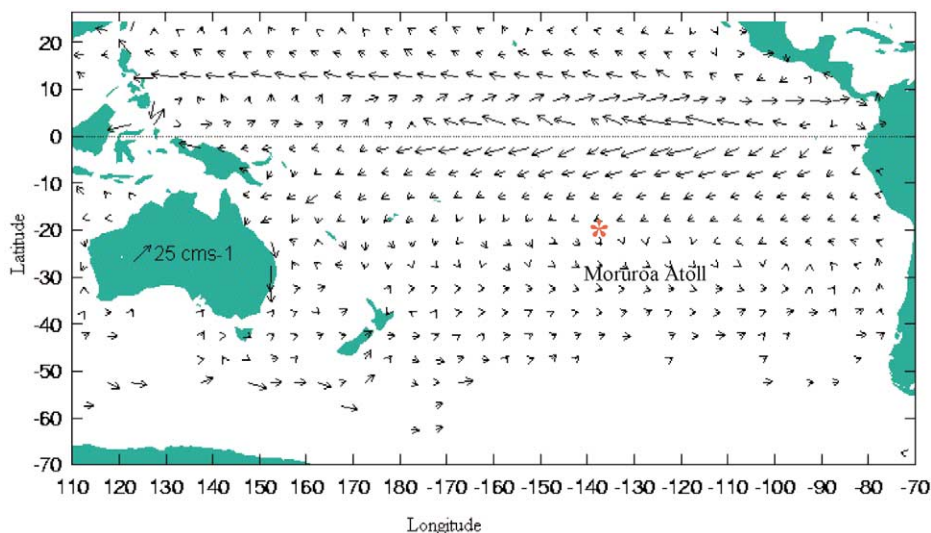


Fig. 2. Observed annual mean velocity estimates at 15 m depth in the South Pacific Ocean (from the Drifter Data Analysis Center of the Global Ocean Observing System, 1996). Velocity data are too sparse in some southern regions to produce a reliable estimate. A vector scale of 25 cm sec⁻¹ is shown over Australia.

year. These near-source currents will advect the initial radionuclide tracer released in the model runs. Current velocities are generally zonal, with eastward flow in the upper 200 m, and westward flow at mid-depth. A southward component is also apparent in the uppermost layer. Seasonal and interannual variations in currents are apparent in the upper 100 m and strongest at the surface. At mid-depths interannual current variability is apparent, whilst seasonal variations remain weak.

2.3. Tracer dispersion model

The effects of advection and dispersion on the radioactive tracer are computed using an off-line tracer model. The model is an adaptation of the GFDL Modular Ocean Model (Bryan, 1969; Cox, 1984; Pacanowski et al., 1991), using its tracer conservation component in combination with other features. The GFDL model is a three-dimensional primitive equation ocean model designed as a flexible tool for ocean and coupled climate modeling. Advection and mixing of the tracer within the model is described by the three-dimensional tracer conservation equation

$$\frac{\partial Q}{\partial t} + u \frac{\partial Q}{\partial x} + v \frac{\partial Q}{\partial y} + w \frac{\partial Q}{\partial z} = K_H \left(\frac{\partial^2 Q}{\partial x^2} + \frac{\partial^2 Q}{\partial y^2} \right) + K_V \left(\frac{\partial^2 Q}{\partial z^2} \right) + Q_S + Q_D \quad (1)$$

where (x, y, z) is Cartesian space, t is time, (u, v, w) the three components of velocity in the (x, y, z) direction, K_H the horizontal mixing coefficient, K_V the vertical mixing coefficient, Q the tracer concentration, Q_S the tracer source, and Q_D the decay/sink of

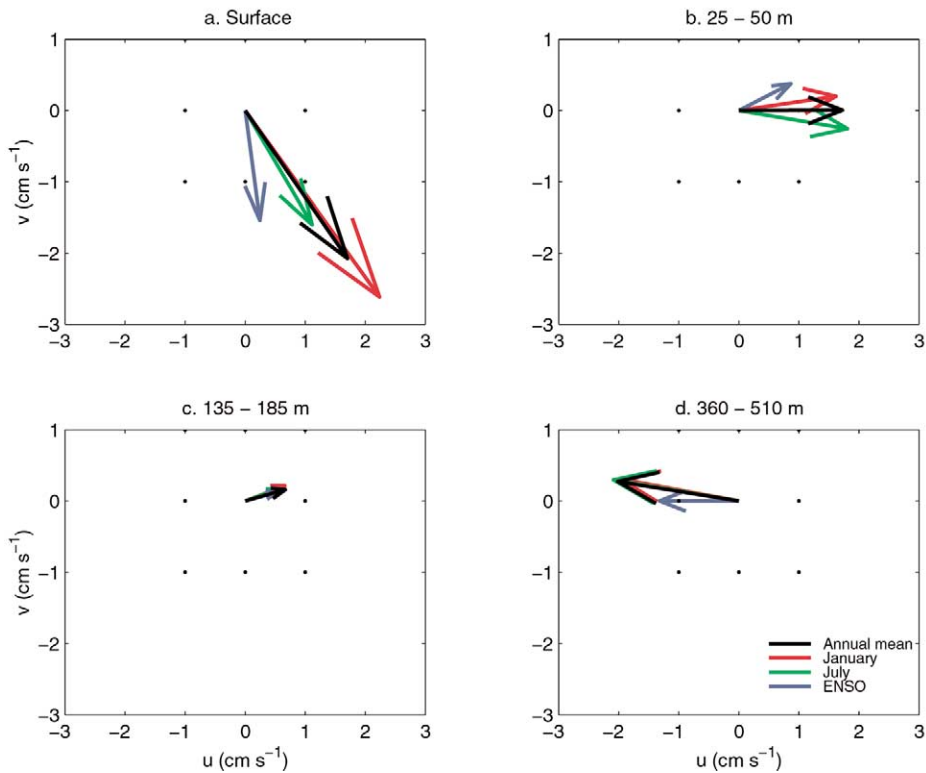


Fig. 3. Horizontal ocean model currents averaged over a 5° grid centered at Moruroa Atoll for the annual mean, and during January, July and ENSO at (a) the surface (0–25 m), (b) 25–50 m, (c) 135–185 m, and (d) 360–510 m depth.

tracer. This conservation equation relates any change in tracer Q to three-dimensional advection and mixing, as well as source/sink terms.

The horizontal components of velocity (u , v) are obtained from the POCM for each grid box and each month of interest. The vertical component of velocity (w) is determined diagnostically from the continuity equation

$$\frac{\partial u}{\partial x} + \frac{\partial v}{\partial y} + \frac{\partial w}{\partial z} = 0. \quad (2)$$

The source term Q_s refers to the release of tracer into the simulated ocean, which has temporal, geographic, and quantitative parameters that are defined separately for each tracer experiment.

A time step of eight hours is adopted in the present study. This value is a compromise between computational efficiency and numerical considerations. It is short enough to avoid ‘overshoots’ of tracer across a single grid box, occurring when the advective distance of tracer exceeds the grid resolution within a single time step. It is also sufficient to avoid excessive numerical diffusion downstream of the tracer signal.

Mixing terms are required within the tracer model to account for physical processes that affect the transport of the tracer which occur at scales below the resolution of the model, and to partly mimic those lost by averaging over a monthly time scale (e.g., transient eddies). The POCM partly resolves ocean dynamical processes at the mesoscale (tens of kilometres in the study domain) and above (e.g., gyres, western boundary currents, deep ocean jets, and so on). This degree of resolution incorporates some eddy advection in prognostic mode. However, the mixing at this scale is unresolved after velocity fields have been averaged. Other ocean dynamical processes that require parameterization include boundary turbulence, tidal mixing, internal wave breaking, vertical convection and velocity shear (England and Oke, 2001). Within the three-dimensional structure of the model, these processes are simply approximated as horizontal and vertical mixing terms (see Eq. (1)).

The parameterization of mixing presents a degree of uncertainty within the tracer model. Horizontal mixing in the ocean is largely dependent upon eddy activity, density structure, and the resultant turbulence and velocity shear created between water masses moving at different velocities. While the POCM partly resolves the mixing created by eddy advection in prognostic mode, our study uses the averaged monthly and annual velocities, which filter out smaller scale transient eddies. As such, the associated turbulence and velocity shear must be parameterized. Regions that experience high levels of eddy activity, such as western boundary currents (WBC) and the Antarctic Circumpolar Current (ACC), will have higher levels of horizontal mixing. Methods for indexing the horizontal mixing coefficient to the degree of eddy activity are a relatively recent ocean modeling development (see, e.g., Rix and Willebrand, 1996; Visbeck et al., 1997), and are yet to be incorporated into this tracer model. We restrict horizontal mixing to a uniform and relatively low value on the basis of some preliminary testing. Model runs were integrated with different values for the horizontal mixing coefficient K_H ranging from 10^2 to 10^7 $\text{cm}^2 \text{sec}^{-1}$. Sensitivity tests undertaken revealed minimal change in simulations once values of K_H fall below 10^5 $\text{cm}^2 \text{sec}^{-1}$. Thus, a value of $K_H = 10^5$ $\text{cm}^2 \text{sec}^{-1}$ was adopted. This is consistent with low eddy activity within the bulk of the study region, as shown by drifting buoy data (Hansen and Poulain, 1996) and sea surface altimetry (Stammer et al., 1996).

Vertical mixing in the surface layer of the ocean is enhanced by wind forcing, which generates breaking waves and turbulence. Below the mixed layer, vertical mixing is of a smaller magnitude. It is influenced by the degree of density stratification and the roughness of the seafloor bathymetry (see, e.g., Toole et al., 1994; Polzin et al., 1997). In the deep ocean, mixing rates are thought to increase due to weaker stratification. Vertical mixing in our tracer model is based on the widely used Bryan and Lewis (1979) profile that approximates mixing as a function of depth. Mixing rates vary from $0.3 \text{ cm}^2 \text{sec}^{-1}$ in the upper ocean to $1.3 \text{ cm}^2 \text{sec}^{-1}$ at depth. This vertical structure is supported by direct estimates of mixing rates in the ocean (Gregg, 1977; Rooth and Ostlund, 1972). The Bryan and Lewis (1979) profile is still used in state-of-the-art climate model simulations (e.g., Manabe and Stouffer, 1996; Hirst et al., 2000). For the purposes of our study, it is a reasonable approximation of mixing in the open South Pacific Ocean near Moruroa Atoll.

3. Experimental design

Moruroa Atoll is part of the Tuamotu Archipelago in French Polynesia. It is located at a longitude of $138^{\circ} 54'$ W, and latitude $21^{\circ} 50'$ S (Fig. 4). The quantity of radioactive material contained within the atoll is not precisely known, but has been estimated to be equivalent to approximately 3.2×10^{17} Bq of ^{137}Cs (Ribbe and Tomczak, 1990). It should be noted that there remains considerable uncertainty in this figure. In view of this, we decided to use an arbitrary unit concentration (1 unit per m^3) as the net release in all experiments. To obtain a prediction of radionuclide concentration under any given scenario therefore requires scaling our model results by the actual quantity (in Bq) released.

The variables incorporated into the tracer release function are (i) the depth of the water column to which the tracer is released, (ii) the duration of the release of the tracer, and (iii) the climatic conditions under which the tracer is released. In all tracer experiments, the model is run over a simulated period of ten years.

3.1. Location of tracer release within the water column

Releases of tracer are simulated at two different depth layers within the water column. The first is to the uppermost depth level of the model, corresponding to the top 25 m of the water column. Such a release could be associated with venting or upwelling of contaminated material through the atoll structure into the lagoon (Rougerie and Wauthy, 1992), or a geological event such as a rock slide affecting the uppermost level of the atoll structure (IAEA, 1998). The second scenario involves a release over the depth range of 360–510 m, corresponding to model depth level nine. This depth range is the location of the karst layer — the interface between the basalt foundation of the atoll and the carbonate upper layer. This layer has been

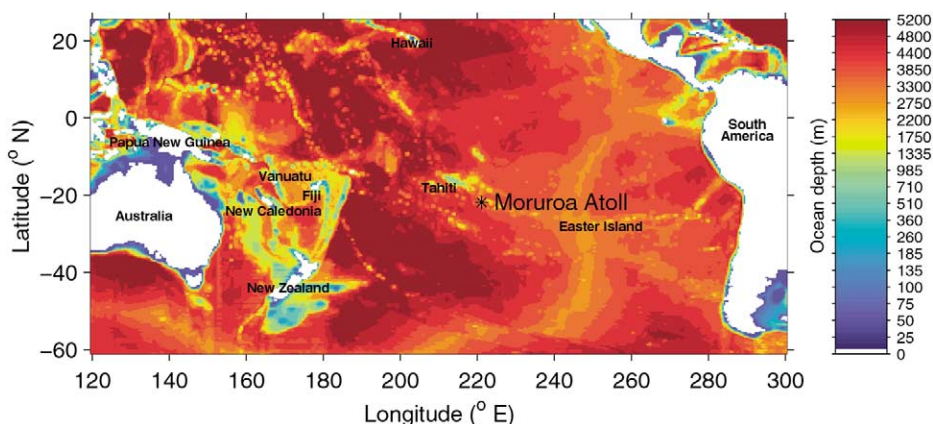


Fig. 4. Bathymetry (m) and continental outline in the tropical and South Pacific regions of the global off-line tracer model. Also highlighted is the location of Moruroa Atoll in French Polynesia.

suggested as a potential conducting medium for the escape of radionuclides coming from the volcanic formations in which weapons tests were conducted (IAEA, 1998).

3.2. Duration of tracer release

Tracer experiments are conducted using two different release periods. The first is an instantaneous (single time-step) release of the entire quantity (1 concentration unit per m^3) of radioactive material into the model grid box in which Moruroa Atoll is located. Such a release may result from a geologically catastrophic incident such as a landslide or earthquake (IAEA, 1998). The second is the gradual release of the same net quantity of material, only over the full duration of ten years. Gradual hydrological processes such as venting or endo-geothermal upwelling (Rougerie and Wauthy, 1992) may be the cause of such a scenario. The duration of ten years is, however, somewhat arbitrary, as determination of an accurate timescale for such processes is not currently feasible (Mittelstaedt et al., 1999).

3.3. Climatic conditions for tracer release

In this study an attempt is made to investigate the possible influence that climate variability can have on the transport of the tracer leakage. Examples of seasonal and interannual climate variability have been incorporated into the model experiments by releasing the tracer into the corresponding seasonal or interannual velocity fields diagnosed from the POCM. To allow a comparison across experiments and with previous studies, each of the above release scenarios is run using the long-term annual mean POCM velocities, as well as three examples of time-varying (u , v) fields.

The annual mean case uses the long-term average of the full twenty years of the POCM velocity field to advect the tracer. Two seasonal climate variability cases are conducted. These use a twelve-monthly cycle of velocity fields averaged from the POCM. Release times are simulated for January and July, corresponding to the summer and winter velocity fields. One simple interannual climate variability case is also conducted. In this experiment the tracer is initially released into a velocity field corresponding to the mean 1982/1983 ENSO circulation (a strong El Niño event). After two years of integration, the model then uses the annual mean velocity field to advect the tracer. The ENSO velocity field used is taken from an average during May 1982 to April 1983, corresponding to the height of the 1982/1983 El Niño (Kiladis and Diaz, 1989).

4. Model results

The results discussed in this section refer to ‘snapshot’ diagrams at selected times in each of the model experiments. Animations of tracer dispersal for each of these experiments can be viewed at the URL: <http://www.maths.unsw.edu.au/~doughaze/projects—moruroa.html>

4.1. Instantaneous release to the surface layer

Using the annual mean velocity fields to advect the tracer, transport is predominantly in an eastward direction with a slight southward component (Fig. 5a). Five years after release, maximum tracer concentration is located between Easter Island and the Chilean coast at 30° S and 270° E. The maximum surface concentrations remain in this region over the rest of the ten-year simulation.

The tracer simulation incorporating a seasonal cycle beginning in January shows the transport of tracer on the surface towards the eastern South Pacific. Unlike the annual mean scenario, however, maximum tracer concentrations remain within 10° E and 2° N of the source (Fig. 5b). The maximum surface concentration remains in close proximity to the release site for the ten years of the simulation.

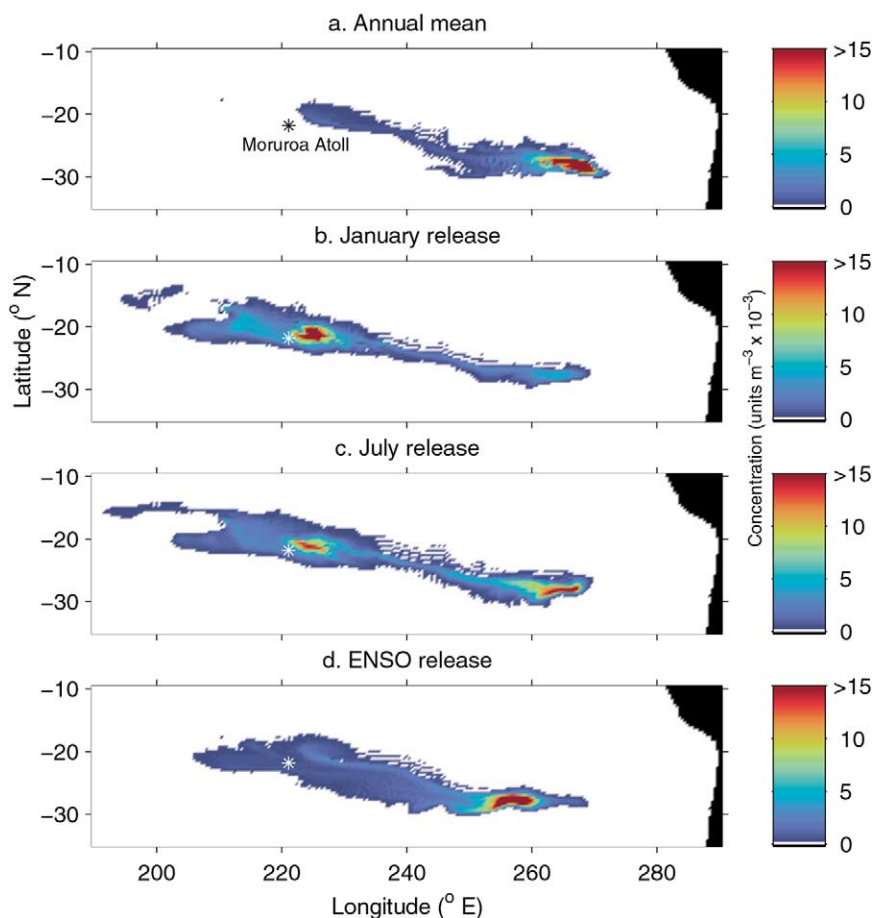


Fig. 5. Tracer concentration (surface layer) relative to an initial release of 1 unit/m^3 after five years in the instantaneous surface release experiments. (a) Annual mean, (b) January, (c) July, and (d) ENSO release simulations.

The July release simulation shows a similar situation to the January release, except that two distinct concentration peaks are apparent. One is in the eastern South Pacific, like the annual mean scenario, and the other is in the source region, as with the January release (Fig. 5c). Again, maximum surface concentration remains in these locations for the duration of the simulation.

The 1982–1983 mean surface velocity fields in the immediate vicinity of Moruroa Atoll are around half the magnitude of the annual mean fields (Fig. 3a). Weaker surface currents during ENSO are linked to weaker geostrophic pressure gradients, due in part to weaker winds that result from reduced tropical atmosphere heat gradients. As a result, the transport of the tracer is much slower in the first two years of the simulation. From the third year on, the annual mean velocity fields advect the tracer, however a lag of about 20° of longitudinal transport is apparent when compared with the annual mean scenario. By the end of the fifth year of the scenario the concentration peak has closed to within 10° of the final location in the annual mean case (Fig. 5d). Surface concentration is at a maximum in the same region as the annual mean surface peak in the eastern South Pacific, where it remains, by the end of the sixth year of the simulation.

Contrary to the direction of predominant surface currents, radioactive material also appears in the surface layer to the west of Moruroa Atoll by the end of the sixth year in all four experiments. This westward transport is the result of vertical mixing between the surface and deeper layers of the model. Once the tracer is mixed to a depth below 135 m, relatively strong subsurface westward currents cause advection of the material across the South Pacific towards Australia (Fig. 6). By the eighth year of simulation, these subsurface currents have transported tracer to the eastern edge of the Australian continental shelf, where the steep topography results in reasonably rapid vertical advection, with the appearance of tracer in the surface layer in the western South Pacific. This upwelling effect is also apparent in the vicinity of many of the Pacific islands. Presumably the convergence of flow at the continental shelf or at the island edge drives a vertical transport upward. The subsurface westward advection of tracer occurs at a similar rate in all four scenarios, however it

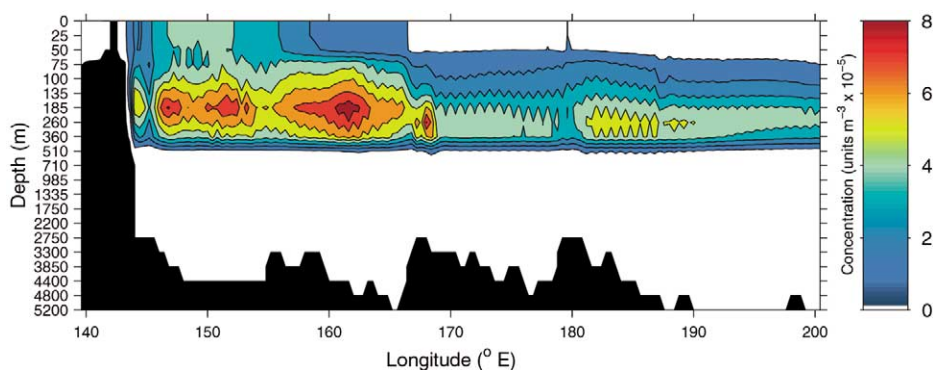


Fig. 6. Zonal cross-section of tracer concentration eight years after 1 unit/m^3 release, integrated over latitudes 11°S – 16°S , from the annual mean simulation in the instantaneous surface release experiment.

shows a lag of two years in the ENSO case compared with the annual mean scenario. This is again due to the reduced current velocities in the initial two years of the ENSO run.

It is worth noting the numerical diffusion apparent in the tracer simulations (see, for example, the wave-like structure in the tracer contours of Fig. 6). Analysis of tracer concentrations downstream of the main plume indicates only weakly negative values (order 3–5% of the main signal). This is typical of tracer advection schemes in ocean GCMs (see, e.g., England and Hirst, 1997). Whilst the negative diffusion values are normally overrun by the spreading tracer plume, some loss of tracer can result.

By the end of the ten-year simulation in all cases, the distribution of radioactive material is widespread throughout the South Pacific Ocean and beyond. The annual mean case is shown in Fig. 7a. Tracer is advected down the east coast of Australia and across the Tasman Sea to New Zealand with the East Australian Current. It has also been transported throughout the equatorial Pacific with the South Equatorial Current and Counter Current, and into the North Pacific. It has also reached the Indian Ocean via the Indonesian throughflow.

The maximum model tracer concentration falls rapidly at similar rates in all four experiments, as mixing and advection processes result in dilution (Fig. 8a). After ten years of simulation time, maximum tracer concentrations range from 3.7×10^{-4} (July release) to 7.8×10^{-4} (annual mean release) concentration units/m³.

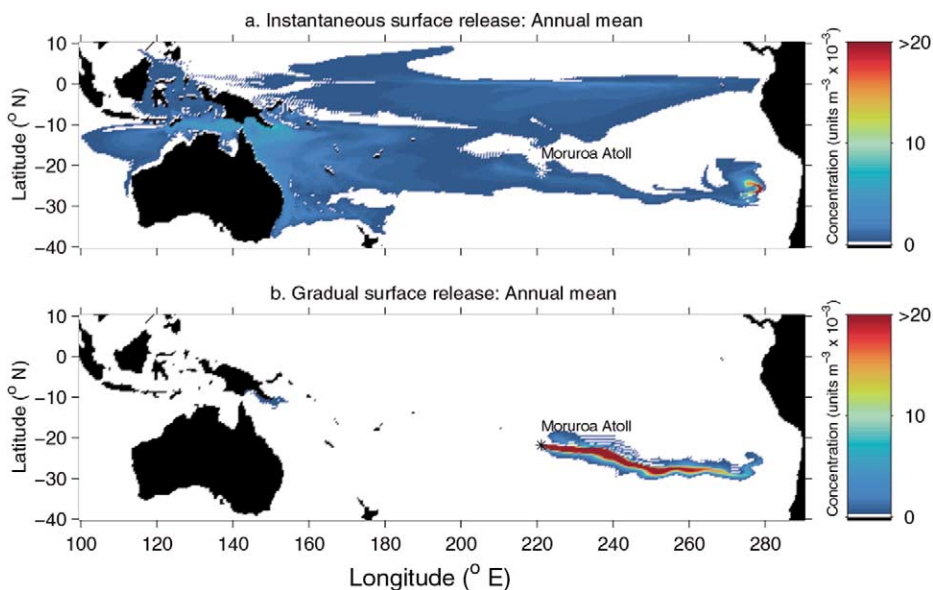


Fig. 7. Tracer concentration in the surface layer relative to a total release of 1 unit/m³ in the annual mean simulations. (a) Ten years after instantaneous surface release, and (b) after ten years of gradual release. Note that in both (a) and (b) there is the same net release of tracer.

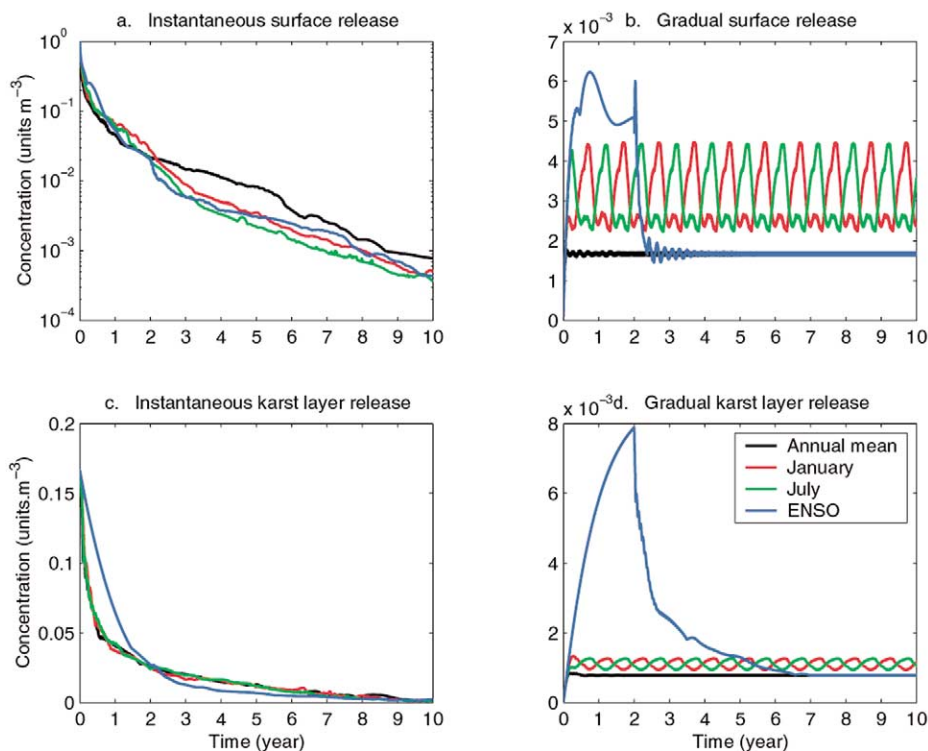


Fig. 8. Maximum tracer concentrations during the ten years of model simulation time. (a) Instantaneous surface release, (b) gradual surface release, (c) instantaneous release to the karst layer, and (d) gradual release to the karst layer. Different concentration scales are used in each panel.

4.2. Gradual release to the surface layer

In contrast to instantaneous release, gradual surface release simulations always show the maximum concentration of tracer to be at, or in the near vicinity of, the source due to the constant input of material (Fig. 7b). Relatively weak large-scale currents in the immediate vicinity of Moruroa prevent direct flushing of the contaminated area. The direction of propagation of the tracer plume is in a generally eastward direction (Fig. 7b). The extent of tracer advection over the ten-year period, and hence the speed of transport, is greatest in the annual mean scenarios. In the seasonal cycle scenarios, eastward propagation is considerably slower, resulting in about 20° less eastward extent by the end of the simulation. This reduction in eastward transport is the result of a recirculation of radioactive material that occurs during the seasonal cycle. After two years in the seasonal release scenarios, a patch of tracer extends northward from the main tracer plume (Fig. 9b,c). This cycle is aliased by the averaging of currents over a single year and so is not apparent in the annual mean and ENSO scenarios (Fig. 9a,d). In the ENSO scenario (Fig. 9d), the reduced local southward surface currents (Fig. 3a) result in greatly reduced advection of tracer from the

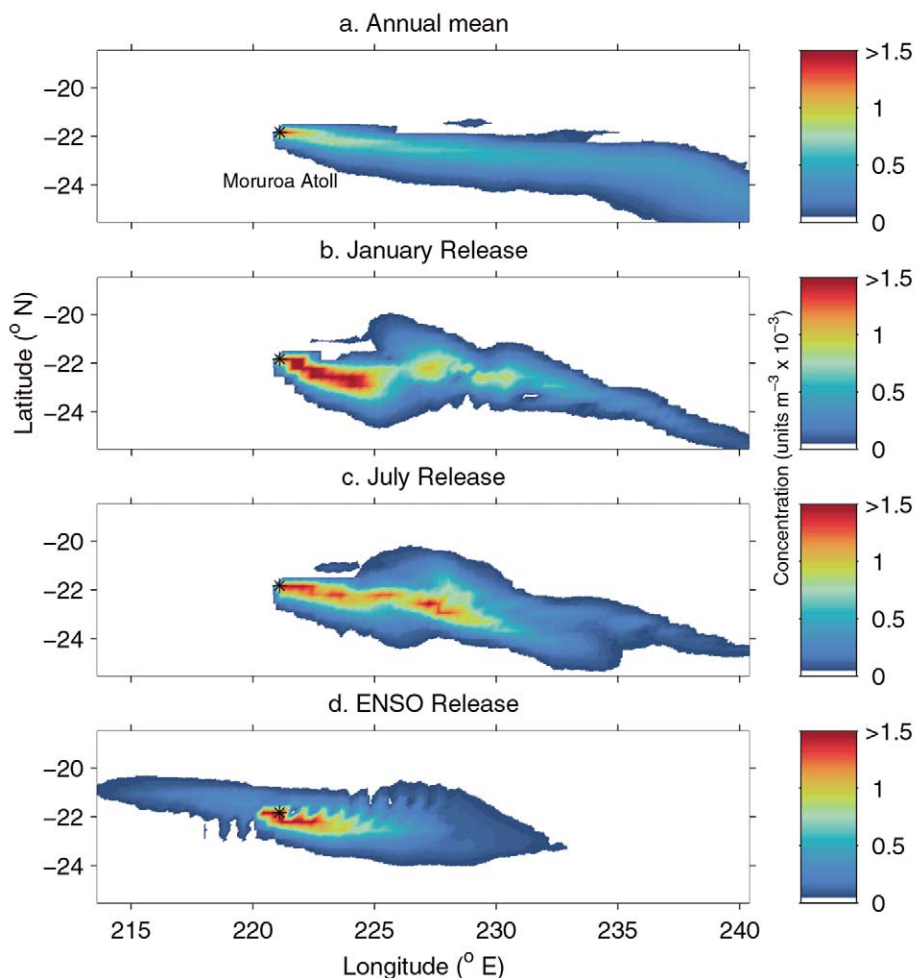


Fig. 9. Tracer concentration (surface layer) after two years in the gradual surface release experiments. (a) Annual mean, (b) January, (c) July, and (d) ENSO release simulations. An asterisk in each panel indicates the location of Moruroa Atoll.

source over the first two years of the simulation, with a predominantly east and west dispersal from the source.

In the ENSO scenario, reduced local currents result in the highest concentration of tracer (6×10^{-3} concentration units/ m^3) in the immediate vicinity of the source (Fig. 8b). Damped fluctuations of maximum tracer concentration in the annual mean and ENSO cases occur due to a return mixing of tracer back into the source grid box. This process continues until equilibrium is established, wherein the amount of tracer released into the source grid box is equal to the amount advected and mixed away. The out-of-phase annual cycle of maximum tracer concentration in the two

seasonal cycle cases occurs as monthly velocity fields advect tracer from the source at different rates.

4.3. Instantaneous release from the karst layer (360–510 meters)

When the tracer is instantaneously released at the depth of the karst layer the annual mean scenario shows it being advected in a westward direction for the first seven years of the simulation. By year six the tracer has reached New Caledonia (Fig. 10a) where it bifurcates, the majority being deflected to the south and only a small proportion to the north. The tracer then continues to flow west in two separate jets. By the seventh year the tracer has reached the coast of Australia between latitudes of 25°S and 18°S. The northernmost component is incorporated into the South Equatorial Current recirculation in the Coral Sea, and by year ten is extending eastward across the Pacific with the South Equatorial Counter Current (Fig. 11a). The more highly concentrated southern component of tracer is rapidly advected down the east coast of Australia with the EAC. By year ten this concentrated signal has crossed the Tasman Sea to the North Island of New Zealand (Fig. 11a).

The seasonal cycle karst layer simulations show the same pattern of initial tracer propagation as the annual mean case (due to reduced seasonal effects at depth). Some differences can be seen after seven years, however, where, upon reaching the steep topography of the continental shelf, faster and more variable ocean currents are encountered (Fig. 10b,c). Throughout the ENSO simulation a similar general transport pattern to the annual mean case is apparent, however in the first two years, due to the reduced current velocities in the ENSO velocity field near Moruroa, the tracer is not advected as far to the west. This lag of about 20° of longitude is sustained through the rest of the simulation (Fig. 10d).

As in the case of the instantaneous surface release experiments, the maximum tracer concentration falls rapidly at similar rates in all four experiments, as mixing and advection processes result in dilution (Fig. 8c). After ten years of the experiment integrations, maximum tracer concentrations range from 1.3×10^{-3} (ENSO release) to 2.3×10^{-3} (January release) concentration units/m³.

4.4. Gradual release from the karst layer (360–510 meters)

Like the instantaneous runs, gradual karst layer release sees tracer advection to the west in all four experiments, with a deflection to the north and south around New Caledonia (Fig. 12). Note, however, that maximum tracer concentrations remain nearer the source in these cases (Fig. 11b, 12). This is due to the continual input of tracer at Moruroa. By year ten, a weak tracer signal has been incorporated into the southward-flowing EAC, and transported across the Tasman Sea to the North Island of New Zealand (Fig. 11b). A small proportion is also advected north into the Coral Sea.

The location of the concentration maximum for the annual mean is at all times in the near vicinity of the source (Fig. 12a), as the input is greater than the local dispersion rate. In the two seasonal cycle simulations, annual pulses of higher con-

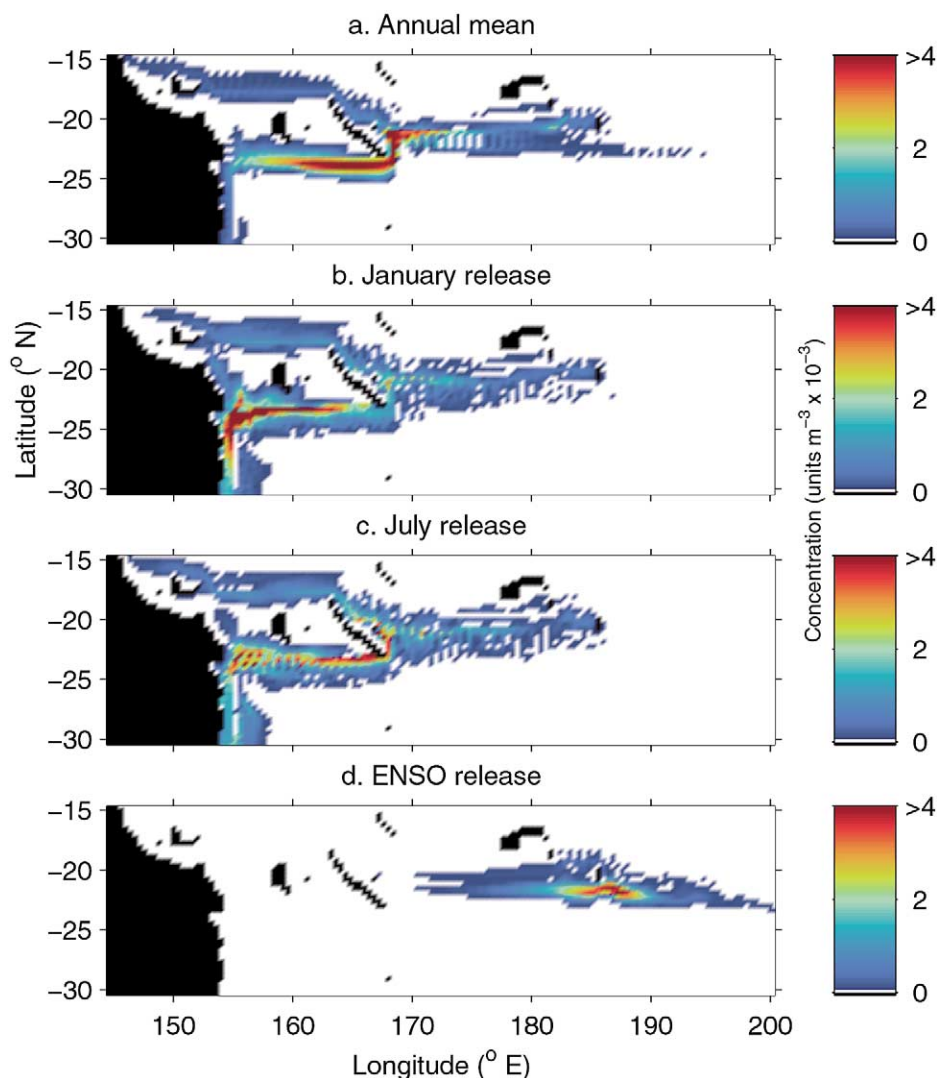


Fig. 10. Tracer concentration (360–510 m depth) relative to an initial release of 1 unit/m³ after seven years in the instantaneous karst layer release experiments. (a) Annual mean, (b) January, (c) July, and (d) ENSO release simulations.

centration of tracer are seen propagating from the source (Fig. 12b,c), indicating that the slight change in current strength over the seasonal cycle at the depth of the karst layer results in downstream variations in tracer concentration. In the ENSO simulation, maximum concentration is located at the source for the duration of the first two years, resulting in a build-up of tracer at Moruroa. With the onset of the faster long-term mean currents in the third year, this accumulated tracer is advected to the west in a pulse of relatively highly contaminated water. After seven years of the

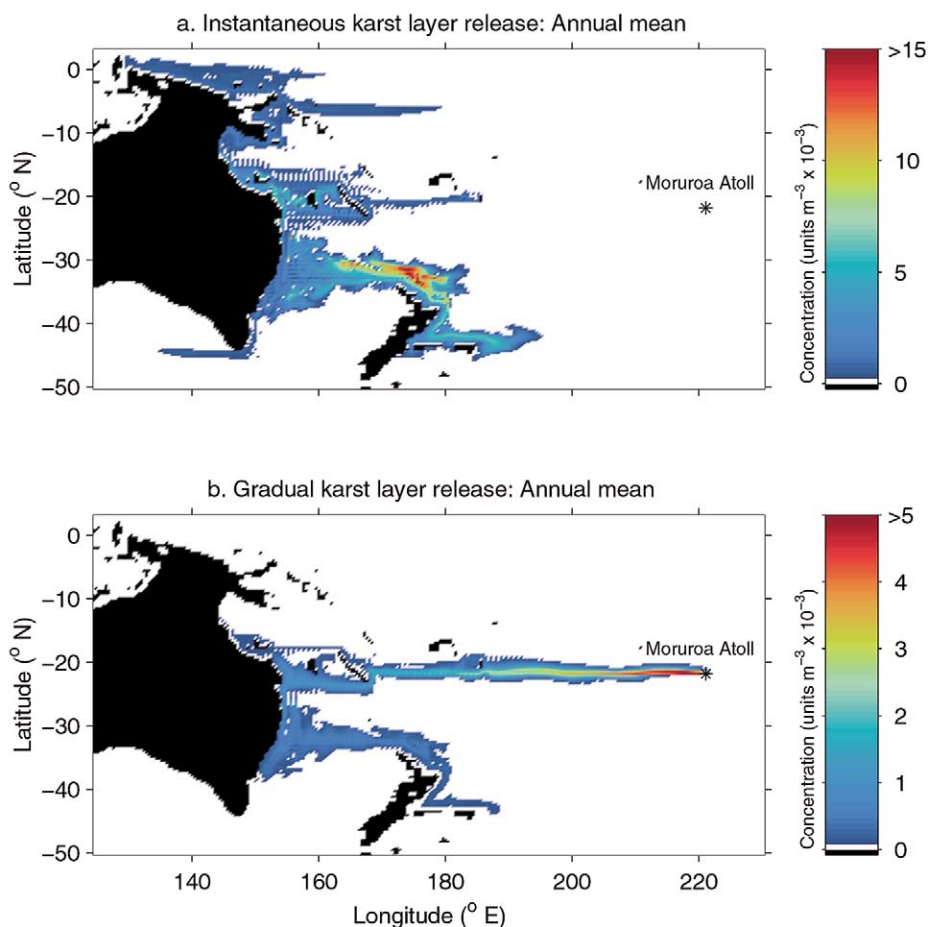


Fig. 11. Tracer concentration (360–510 m depth) relative to a total release of 1 unit/m^3 after ten years from the annual mean simulations in the karst layer release experiments. (a) Instantaneous release, (b) gradual release. Note that in both (a) and (b) there is the same net release of tracer.

ENSO simulation, the maximum concentration of radionuclides is located 40°W of the source in the region of Tonga (Fig. 12d). By eight years the pulse has dissipated and the maximum tracer concentration is again located at the source.

The maximum tracer concentrations in the karst layer gradual-release experiments are shown in Fig. 8d. A very rapid increase in maximum concentration is apparent over the first few years as tracer is mixed back into the source grid boxes, which is highest for the ENSO simulation (8×10^{-3} concentration units/ m^3) due to the reduced local current speeds. Peak ENSO simulation concentrations decrease and are finally equal to the annual mean simulation maximum (0.8×10^{-3} concentration units/ m^3) after seven years of run time. The seasonal cycle simulations show out-of-phase annual fluctuations corresponding to the variable current velocities during the course of a year (Fig. 8d).

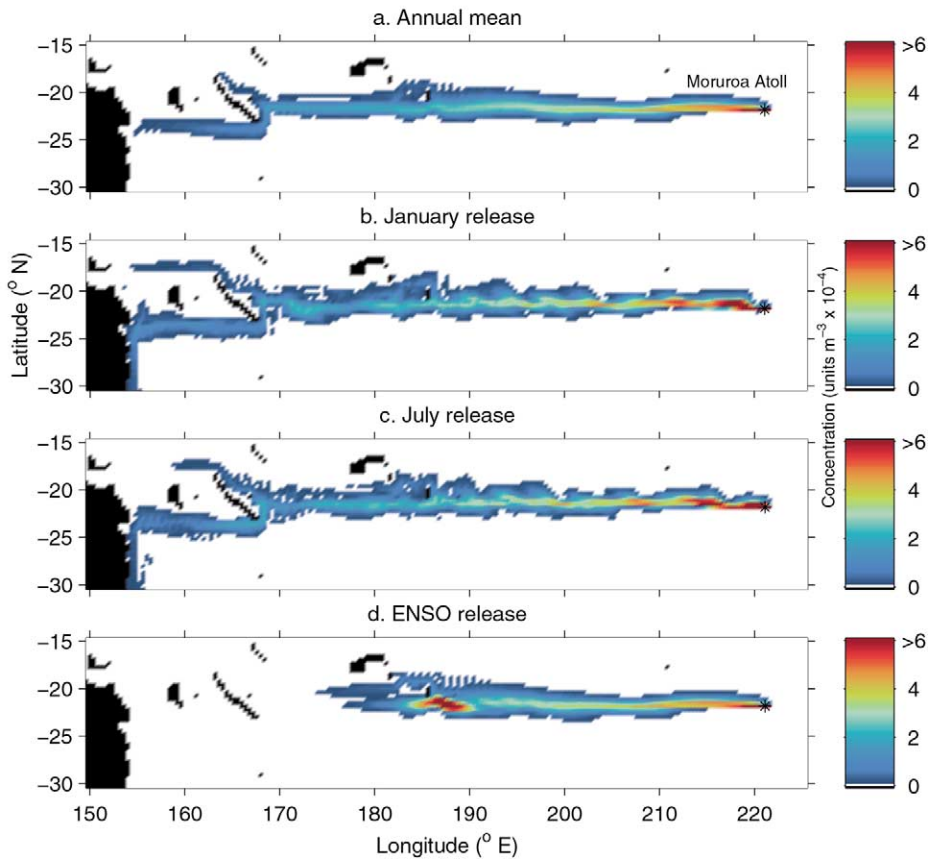


Fig. 12. Tracer concentration (360–510 m depth) after seven years in the gradual karst layer release experiments. (a) Annual mean, (b) January, (c) July, and (d) ENSO release simulations.

5. Discussion

The results of the simulations conducted in this study provide the most extensive understanding of the consequences of a radioactive leak from Moruroa Atoll to date. This study has made use of some of the best ocean-modeling tools currently available, including output from a global eddy-permitting ocean model. The duration and depth of tracer release to the water column have shown important differences in the ultimate fate of the radioactive material. The inclusion of natural variability into the simulations has been particularly illuminating, highlighting the difference in both pathways of tracer advection and magnitude of tracer concentration under different climate scenarios (discussed in the next section). Previous studies of radioactive tracer dispersion from Moruroa Atoll have assumed constant velocity fields, and generally adopt coarse-resolution models within limited domains. We directly compare the results of our study with two previous models (Ribbe and Tomczak, 1990,

Lazar and Rancher, 1999) in the following section. Finally, suggested improvements for future studies are discussed in the final section.

5.1. Influence of ocean current variability on tracer advection and concentration

This study has demonstrated the importance of the inclusion of seasonal and interannual variations in ocean model velocity fields for the fate of radionuclide pollutants in the South Pacific Ocean. No previous study considered this factor beyond the regional scale, despite evidence for seasonal and interannual ocean current variability.

When seasonally varying velocities are incorporated into the instantaneous surface-release experiments from Moruroa Atoll, the variable ocean currents greatly reduce the eastward transport. The cycling of the direction of velocity a few degrees to the east of the source acts to maintain the maximum surface concentration of radioactive material within French Polynesia. The transport towards South America seen in the annual mean scenario is still apparent, however it is much reduced with a seasonal velocity field. This seasonal transport result is in contrast to the constant velocity experiments of Lazar and Rancher (1999) and Mittelstaedt et al. (1999), who find maximum radionuclide concentrations in the eastern South Pacific.

The importance of the time of release within the seasonal cycle also influences the ultimate fate of the radioactive material. In a winter release, when south-eastward surface currents are weaker at the release site, a greater amount of tracer is able to be vertically mixed to depths of 25–75 m. This reduces the amount of tracer that is contained within the surface current cycle, allowing a greater proportion to advect to the east. The weakening of currents in the upper six depth levels of the model seen during ENSO is also important for the resultant radionuclide advection, as eastward transport is much slower while the ENSO fields are active.

Subsurface westward advection of tracer in the subtropical gyre is also influenced by the inclusion of a mean monthly cycle of velocity fields. During the seasonal runs, larger quantities of tracer are retained in French Polynesia, resulting in a greater degree of vertical mixing to the levels of westward currents at depths below 260 m. Radioactive material then reaches the Australian continent one year earlier than in the annual mean scenario.

The results from the scenario of instantaneous karst layer release show sensitivity to interannual current variability, however seasonal variability, as would be expected at this depth, has much less effect. Little difference can be seen between the releases under monthly cycle advection and annual mean advection until the strong and variable currents off the east coast of Australia are encountered. Despite the lack of direct current observations below the surface mixed layer (0–150 m) in the central South Pacific, this aspect of the model agrees with the general picture of the wind-driven subtropical anticyclonic gyre. The gyre occupies the upper 400 m of the ocean and is decreasingly responsive with depth to seasonal variations, such as trade winds and cyclones. Below this depth, the westward flowing Antarctic Intermediate Water is found, which is not influenced by local atmospheric conditions, but driven by

longer-term and larger-scale thermohaline forces and geostrophic effects (see, for example, Tomczak and Godfrey, 1994).

When tracer is released under ENSO velocity fields and compared with the annual mean simulations, a different scenario is revealed. Tracer advected under ENSO velocity fields is transported much more slowly from the source when compared with the annual mean release. This can be partially explained by the reduction in the anticlockwise momentum of the subtropical gyre under ENSO conditions, most obviously demonstrated by the dramatic reduction in the velocity of the equatorial currents (Tomczak and Godfrey, 1994). This reduction is due to weaker winds caused by reduced meridional sea surface temperature (SST) gradients during ENSO years.

Whilst the direction and speed at which radionuclides are transported from Moruroa Atoll differ when ocean current variability is included in the instantaneous release experiments, the magnitude of the maximum concentration decays at similar rates. This is due largely to the relatively weak ocean currents in the central South Pacific, meaning that background mixing determines to a large extent the size of the maximum tracer signal.

Ocean current variability has a direct effect on the local concentration of radioactive material in the gradual release scenarios. When ocean currents in the release region are stronger, concentration is reduced. This is a simple relationship between the rate of tracer input, and the rate at which tracer is advected and mixed away from the source. At all times within the seasonal cycle runs, maximum tracer concentrations are greater than those in the annual mean scenarios. The greatest concentrations modeled are associated with the weakest local currents; these occur in the first two years of the ENSO scenarios.

5.2. Comparison with previous studies

Our simulation of the instantaneous release of radionuclides to the surface model layer from Moruroa Atoll can be compared with two previous studies that have modeled the same scenario (RT90, and LR99). RT90 estimate the quantity of radioactive material contained within Moruroa to be equivalent to 3.2×10^{17} Bq of ^{137}Cs . They then simulate a ‘worst case’ scenario in which this entire radioactive inventory is released instantaneously to the surface layer, the model is then run for ten years. This simulation was repeated by LR99 using a higher-resolution model with a larger domain. The results of our study, with 1 unit/m^3 release concentration, can be scaled so that the initial tracer release is equal to that of the previous studies. This has been calculated by dividing the estimated quantity of radioactive material (3.2×10^{17} Bq) by the release grid box volume ($\sim 41 \text{ km} \times 41 \text{ km} \times 25 \text{ m} = 4.2 \times 10^{10} \text{ m}^3$) to obtain a scale factor of $7.6 \times 10^6 \text{ Bq m}^{-3}$.

Fig. 13 shows a schematic diagram of the direction of propagation of the maximum tracer concentration in the three simulations using the annual mean velocity fields. It can be seen that there is general agreement between our study and that of LR99, while the spread of tracer in RT90 is in the opposite direction. RT90 found the propagation of maximum surface tracer concentration to be westward, while LR99 and our simulations indicate primarily south-eastward transport.

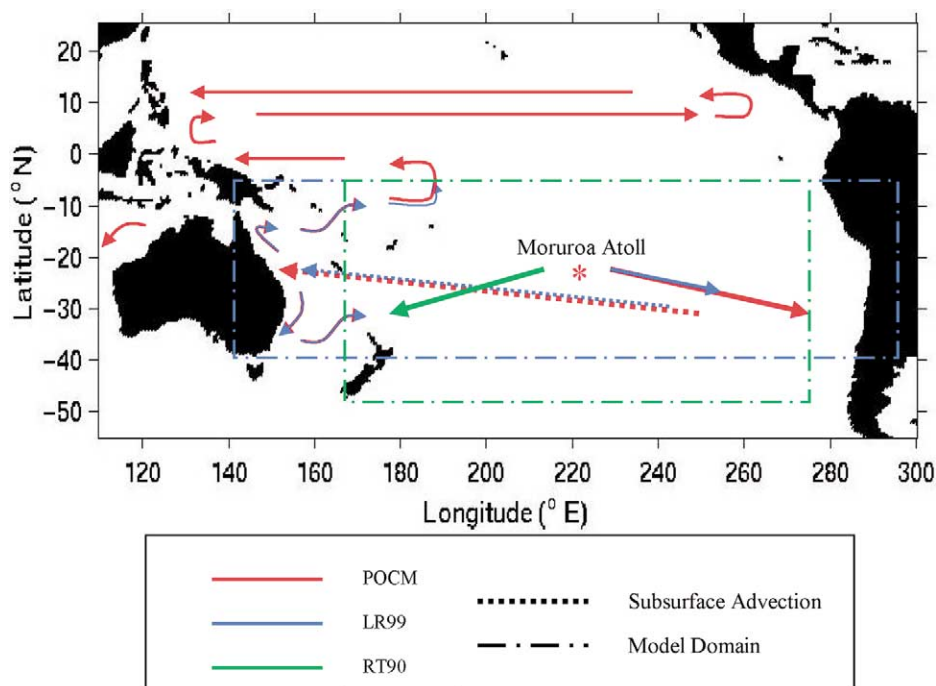


Fig. 13. Schematic diagram showing Moruroa tracer propagation in the South Pacific Ocean in our study using the POCM, as compared to the previous studies of LR99 and RT90. Vectors show tracer spread over a ten-year period, with bold arrows indicating the peak concentration pathway. Also shown are the limited model domains of RT90 and LR99.

The dramatic disagreement in tracer advection direction between our study and that of RT90 can be attributed to the very coarse resolution of their model. The longitude–latitude resolution in RT90 is 3.75° by 4.5° compared with 2° by $\sim 1^\circ$ in LR99 and 0.4° by $\sim 0.2^\circ$ in our model. The RT90 low resolution is unable to capture many of the features of the ocean circulation, with flow at the surface near Moruroa Atoll simply a broad slow flux in the subtropical gyre. Their model uses only 12 depth levels — the surface level of which is 50 m thick — compared with 20 levels in this study (with surface level 25 m thick) and 30 levels in LR99 (with surface level 12.5 m thick). The coarse RT90 vertical resolution in the upper ocean is unable to realistically represent the vertical structure of the gyre circulation in the South Pacific Ocean. An additional factor is the surface forcing fields, which in RT90 are derived from a coarse-grid atmospheric model. Our velocity fields, in contrast, come from a model forced by ECMWF model reanalyses, which capture storm tracks and weather-scale variability in the atmosphere. This leads to increased horizontal structure in the surface flow fields in the POCM.

The results of our study show that the location of the tracer concentration peak after ten years is 30° further to the east and 10° further to the south when compared to the simulation of LR99. Both models show the tracer peak to be located within

the convergence region in the eastern South Pacific, however the higher resolution of the POCM shows some subtle currents persisting with eastward flow that are not apparent in the LR99 circulation model. The subsurface advection of tracer that results in upwelling off the east coast of Australia is seen in both models.

The maximum tracer concentration over time shows significant differences between the three model studies (Fig. 14). Our maximum concentrations are a factor of 100 greater than those in LR99 and RT90. It should be noted, however, that initial concentrations are different in the three studies due to the different model resolutions, such that larger volume elements result in lower initial concentrations. This difference in initial concentration will clearly influence the resultant maximum concentration of tracer over time. The initial difference in release concentration is a factor of 10 and 100 lower in the LR99 and RT90 studies, respectively, when compared with our model. The small size of Moruroa Atoll is not specifically resolved by any of the three models, so it may be assumed that in all cases the initial concentration is underestimated as it is instantaneously mixed over the source grid box. The RT90 and LR99 studies therefore impose a much greater degree of dilution to the tracer prior to any incorporation of physical ocean processes. The *final* maximum concentration in our study turns out to be only a factor of 10 less than the *initial* concentration in RT90.

The initial dilution difference between the three model cases does not explain all of the differences seen in maximum concentrations. When maximum concentration (Q_{max}) is divided by the initial concentration (Q_0) and plotted against time, our model still shows significantly higher concentrations throughout the simulation compared with LR99 and RT90 (Fig. 14b). The horizontal resolution of the three models provides a second important explanation for the large difference in Q_{max}/Q_0 . Neither RT90 nor LR99 were of sufficient horizontal resolution to resolve many of the smaller-scale features of ocean circulation such as narrow jets and quasi-stationary

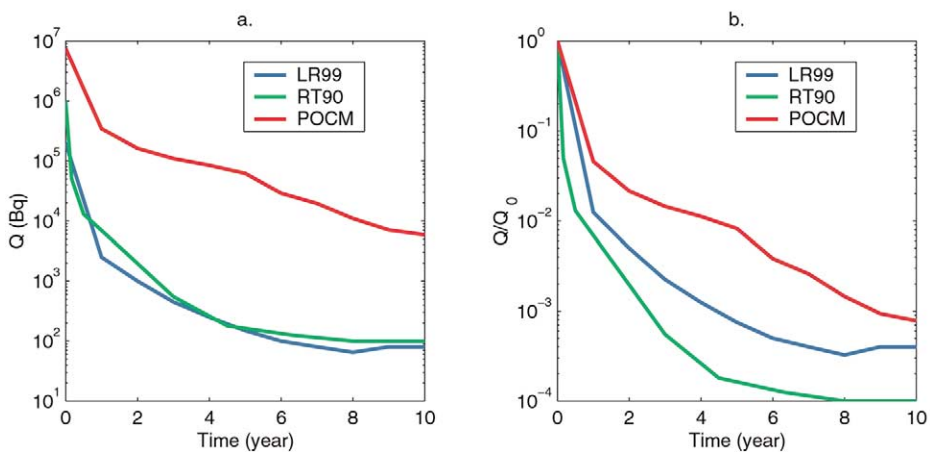


Fig. 14. Comparison of (a) maximum tracer concentration (Q) (in Bq), and (b) maximum concentration divided by initial concentration (Q/Q_0) for the present study (POCM), as compared to LR99 and RT90.

eddies. Thus, the majority of water-mass mixing is parameterized, and advection fields are relatively broad and sluggish, particularly in the case of RT90. The finer resolution of the POCM is better able to capture the advective components of ocean dynamics, and thus reduce the need for their parameterization. It is likely that our horizontal mixing coefficient is a little too low for particularly high-energy areas of the ocean, such as the EAC. However, the low-energy environment of the majority of the South Pacific Ocean is reasonably well parameterized by our mixing term. In contrast, horizontal mixing has been overestimated in previous studies, particularly RT90. The results of our study provide a more accurate estimate of tracer dispersion from Moruroa Atoll.

The final important difference between the results of the three studies concerns the model domain. Our study has utilized a global ocean model, effectively without artificially imposed boundaries, and therefore does not require the inclusion of side boundary conditions. The RT90 and LR99 models were both restricted to South Pacific Ocean domains. The results of our study show the tracer being advected beyond the boundaries of both these earlier studies within the ten-year integration (Fig. 13), a situation that is impossible to account for in the earlier models.

If the RT90 estimate of 3.2×10^{17} Bq of ^{137}Cs is an accurate guide to the amount of contaminated material contained within Moruroa, our study suggests that the resultant contamination to the local marine environment would remain as high as 10,000 times greater than the current background concentration (0.5 Bq m^{-3} averaged over 2000 m depth (Povinec et al., 1999) ten years after a catastrophic geological event.

5.3. Improvements in future studies

We have demonstrated the importance of ocean current variability and high model resolution in tracer release modeling studies. There are, however, improvements that could be made. An ideal simulation would combine seasonal and interannual variability into a single model run. This could involve superimposed monthly and interannual cycles, or real-time forecasting. In the case of the ENSO climate cycle this would account for La Niña, El Niño and the transition between these events. Releases could be simulated at times throughout the interannual and seasonal cycles. Such a study would require numerous integrations and is beyond the scope of our initial goals. There would likely be more variability in the possible fate of radioactive material in the marine environment with a greater variety of ocean circulation scenarios. Our study has demonstrated the importance of seasonal to interannual variations without covering the full range of possible cycles.

Improvements to the off-line tracer model used in this study could also be made. In particular, the representation of subgrid-scale mixing would be greatly improved with the incorporation of a more physically realistic parameterization of horizontal mixing, such as along-isopycnal mixing and a bolus transport term (e.g., Gent and McWilliams, 1990). This would be particularly useful in improving the prediction of tracer fate in eddy-rich regions such as the ACC and EAC, where ocean currents are swift and variable. Ideally, the model would also include a simple wind-driven

mixing scheme for representing enhanced upper-ocean vertical mixing in the presence of strong winds.

6. Conclusions

This study has provided insight into the potential fate of radioactive contamination released into the South Pacific marine environment. Our results can be scaled to a real-world scenario by multiplying the model data by the actual release concentration (see details in Sect. 5.2). Releases of large quantities of radionuclides from Moruroa Atoll could have large-scale and long-term consequences, with elevated levels of radioactivity for Pacific Island, South American and Australasian nations within ten years of initial release.

The fate of leaked radioactive material from the geological structure of Moruroa Atoll varies as a function of the release depth and rate, and the oceanic climate into which it is released. Instantaneous surface leakage remains most highly concentrated in French Polynesia when seasonal variability is incorporated into the tracer model, in contrast to previous model studies using longer-term average velocity fields (wherein maximum concentrations are advected towards the south eastern Pacific). Vertical mixing, subsurface transport, and topographically induced upwelling also influence the fate of contaminants released from Moruroa. These lead to the appearance of radionuclides in the coastal waters of Australia within seven years of tracer release. The concentration of radioactive material, if gradually released through hydrogeological processes, remains highest near the source. The concentration is dependent upon the strength of currents, and is thus closely linked to ocean circulation variability. The worst case scenario for the nations in the vicinity of French Polynesia would be an instantaneous release during an ENSO year. This would see weak local currents having only a small effect on dispersing the pollutant. While previous studies have suggested that maximum radionuclide concentrations would be found in the relatively unpopulated eastern South Pacific following an instantaneous release, we have shown that seasonal variability can result in maximum concentrations remaining within French Polynesia.

Acknowledgements

Robin Tokmakian kindly provided the global POCM velocity data used in this study. This research was supported in part by the Australian Research Council. Observational velocity data shown in Fig. 2 were provided by the Drifter Data Analysis Center of the Global Ocean Observing System (GOOS) at NOAA/AOML, Miami, Florida.

References

- Bryan, K., 1969. A numerical method for the study of the circulation of the World Ocean. *Journal of Computational Physics* 3, 347–376.
- Cox, M.D. (1984). A primitive equation, three-dimensional model of the ocean. Geophysical Fluid Dynamics Laboratory Ocean Group Technical Report 1, 143 pp., Princeton, New Jersey.
- Bryan, K., Lewis, L.J., 1979. A water mass model of the World Ocean. *Journal of Geophysical Research* 84, 2503–2517.
- Deleersnijder, E., Tartinville, B., Rancher, J., 1997. A simple model of the tracer flux from the Mururoa lagoon to the Pacific. *Applied Mathematics Letters* 10, 13–17.
- England, M.H., Oke, P., 2001. Ocean modeling and prediction. In: Leslie, L., Peng, P., Shao, Y. (Eds.), *Environmental modelling and prediction*. Springer-Verlag, pp. 125–171.
- England, M.H., Hirst, A.C., 1997. Chlorofluorocarbon uptake in a World Ocean model. 2. Sensitivity to surface thermohaline forcing and subsurface mixing parameterisation. *Journal of Geophysical Research* 102, 15709–15731.
- Gent, P.R., McWilliams, J.C., 1990. Isopycnal mixing in ocean circulation models. *Journal of Physical Oceanography* 20, 150–155.
- Gregg, M.C., 1977. Variations in the intensity of small-scale mixing in the main thermocline. *Journal of Physical Oceanography* 7, 436–454.
- Hansen, D.V., Poulain, P.M., 1996. Quality control and interpolation of WOCE/TOGA drifter data. *Journal of Atmospheric and Oceanic Technology* 13, 900–909.
- Hirst, A.C., O'Farrell, S.P., Gordon, H.B., 2000. Comparison of a coupled ocean-atmosphere model with and without oceanic eddy-induced advection. Part I: Ocean spinup and control integrations. *Journal of Climate* 13, 139–163.
- IAEA (1998). *The Radiological Situation of the Atolls of Mururoa and Fangataufa*. 53pp., IAEA, Vienna.
- Kiladis, G.N., Diaz, H.F., 1989. Global climatic anomalies associated with extremes in the Southern Oscillation. *Journal of Climate* 2, 1069–1090.
- Lazar, A., Rancher, J., 1999. Simulation of radionuclide dispersion in the Pacific Ocean from Mururoa Atoll. *Journal of Environmental Radioactivity* 43, 31–49.
- MacLellan, N., Chesneaux, J., 1998. *After Moruroa: France in the South Pacific*. Ocean Press, Australia.
- Manabe, S., Stouffer, R.J., 1996. Low-frequency variability of surface air temperature in a 1000-year integration of a coupled ocean–atmosphere–land surface model. *Journal of Climate* 9, 376–393.
- Mittelstaedt, E., Osvath, I., Povinec, P., Togawa, O., Scott, M., 1999. Transport of radionuclides from the Mururoa and Fangataufa atolls through the marine environment. *The Science of the Total Environment* 237/238, 301–309.
- Pacanowski, R.C., Dixon, K.W., Rosati, A. (1991). *The Geophysical Fluid Dynamics Laboratory Modular Ocean Model users guide*, Geophysical Fluid Dynamics Laboratory Ocean Group Technical Report 2, 46 pp., Princeton, New Jersey.
- Polzin, K.L., Toole, J.M., Ledwell, J.R., Schmitt, R.W., 1997. Spatial variability of turbulent mixing in the abyssal ocean. *Science* 276, 93–96.
- Povinec, P.P., Woodhead, D., Blowers, P., Rachel, B., Cooper, M., Chen, Q., Dahlgard, H., Dovlete, C., Fox, V., Froehlich, K., Gastaud, J., Groning, M., Hamilton, T., Ikeuchi, Y., Kanisch, G., Kruger, A., Kwong, L.L.W., Matthews, M., Morgenstern, U., Mulsow, S., Pettersson, H., Smedley, P., Taylor, B., Taylor, C., Tinker, R., 1999. Marine radioactivity assessment of Mururoa and Fangataufa atolls. *The Science of the Total Environment* 237/238, 249–267.
- Reid, J.L., 1986. On the total geostrophic circulation of the South Pacific Ocean: flow patterns, tracers, and transports. *Progress in Oceanography* 16, 1–61.
- Rix, N.H., Willebrand, J., 1996. Parameterization of mesoscale eddies as inferred from a high-resolution circulation model. *Journal of Physical Oceanography* 26, 2281–2285.
- Ribbe, J., Tomczak, M., 1990. An impact assessment for the French nuclear sites in French Polynesia. *Marine Pollution Bulletin* 21, 536–542.
- Rooth, C.G., Ostlund, H.G., 1972. Penetration of tritium into the Atlantic thermocline. *Deep-Sea Research* 19, 481–492.

- Rougerie, F., Wauthy, B., 1992. Geothermal endo-upwelling: a solution to the reef nutrient paradox? *Continental Shelf Research* 12, 785–798.
- Semtner, A., Chervin, R., 1992. Ocean general circulation from a global eddy-resolving model. *Journal of Geophysical Research* 97, 5493–5550.
- Stammer, D., Tokmakian, R., Semtner, A., Wunsch, C., 1996. How well does a quarter-degree global circulation model simulate large-scale oceanic observations? *Journal of Geophysical Research* 101, 25779–25811.
- Tartinville, B., Deleersnijder, E., Rancher, J., 1997. The water residence time in the Mururoa atoll lagoon: a three-dimensional model sensitivity analysis. *Coral Reefs* 16, 193–203.
- Tomczak, M., Godfrey, J.S., 1994. *Regional Oceanography: An Introduction*. Elsevier, New York.
- Tomczak, M., Herzfeld, M., 1998. Pollutant pathways between Mururoa and other Polynesian islands, based on numerical model trajectories. *Marine Pollution Bulletin* 36, 288–297.
- Toole, J.M., Polzin, K.L., Schmitt, R.W., 1994. Estimates of diapycnal mixing in the abyssal ocean. *Science* 264, 1120–1123.
- Visbeck, M., Marshall, J., Haine, T., Spall, M., 1997. On the specification of eddy transfer coefficients in coarse resolution ocean circulation models. *Journal of Physical Oceanography* 27, 381–402.